

Hydrodynamic thickening of lubricating fluid layer beneath sliding mesothelial tissues

Judy L. Lin^a, Taraneh Moghani^a, Ben Fabry^b, James P. Butler^b, Stephen H. Loring^{a,*}

^aDepartment of Anesthesia and Critical Care, Beth Israel Deaconess Medical Center and Harvard Medical School, Boston, MA 02215, USA

^bMolecular and Integrative Physiological Sciences, Harvard School of Public Health, 665 Huntington Ave, Boston, MA, USA

Accepted 28 January 2008

Abstract

The delicate mesothelial surfaces of the pleural space and other serosal cavities slide relative to each, lubricated by pleural fluid. In the absence of breathing motion, differences between lung and chest wall shape could eventually cause the lungs and chest wall to come into contact. Whether sliding motion keeps lungs and chest wall separated by a continuous liquid layer is not known. To explore the effects of hydrodynamic pressures generated by mesothelial sliding, we measured the thickness of the liquid layer beneath the peritoneal surface of a 3-cm disk of rat abdominal wall under a normal stress of 2 cm H₂O sliding against a glass plate rotating at 0–1 rev/s. Thickness of the lubricating layer was determined microscopically from the appearance of fluorescent microspheres adherent to the tissue and glass. Usually, fluid thickness near the center of the tissue disk increased with the onset of glass rotation, increasing to 50–200 μm at higher rotation rates, suggesting hydrodynamic pumping. However, thickness changes often differed substantially among tissue samples and between clockwise and counter-clockwise rotation, and sometimes thickness decreased with rotation, suggesting that topographic features of the tissue are important in determining global hydrodynamic effects. We conclude that mesothelial sliding induces local hydrodynamic pressure gradients and global hydrodynamic pumping that typically increases the thickness of the lubricating fluid layer, moving fluid against the global pressure gradient. A similar phenomenon could maintain fluid continuity in the pleural space, reducing frictional force and shear stress during breathing.

© 2008 Elsevier Ltd. All rights reserved.

Keywords: Respiratory mechanics; Pleural space; Elastohydrodynamic lubrication; Epifluorescence microscopy; Rat

1. Introduction

With each breath, the pleural surfaces of lungs and chest wall slide past each other, lubricated by pleural fluid. The nature of the physical interaction between the pleural surfaces of lung and chest wall has been controversial. Agostoni and D'angelo (1991) have argued that the difference between estimated surface pressure over the lungs and fluid pressure is evidence for solid-to-solid contact. The necessity for contact was challenged by Lai-Fook (1987), Lai-Fook and Rodarte (1991, 2004), who suggested that fluid pressure is actually equal to surface pressure and proposed that a continuous fluid layer

separates the pleural surfaces of lung and chest wall, lowering shear stress during breathing.

Several groups have explored the tribological behavior of sliding mesothelial tissues to deduce the presence and importance of contact between the sliding surfaces. Tribological behavior is commonly divided into four lubrication regimes: boundary lubrication, mixed lubrication, elastohydrodynamic lubrication, and fully developed hydrodynamic lubrication (Dowson, 1969; Adamson, 1982). In boundary lubrication, which occurs at lower sliding speeds, asperities (protuberances) on the sliding surfaces are in contact or separated by extremely thin films of lubricant, and hydrodynamic pressures are unimportant in supporting the normal load. In this regime, frictional force is relatively invariant with velocity. At the highest sliding velocities in hydrodynamic lubrication, fluid thickness is much greater than the amplitude of the surface

*Corresponding author. Tel.: +1 617 667 3092; fax: +1 617 667 1500.
E-mail address: sloring@bidmc.harvard.edu (S.H. Loring).

roughness, hydrodynamic pressure bears the entire load, and frictional force rises with velocity. In elastohydrodynamic lubrication at intermediate sliding speeds, asperities are deformed by hydrodynamic pressures and do not come into contact because they are separated by a continuous layer of lubricant. In this regime (and in mixed lubrication, which has the features of both boundary and elastohydrodynamic lubrication), frictional force typically decreases within a range of increasing velocity. Thus, each lubrication regime has its own characteristic frictional behavior. Early tribological studies of pleural tissues measured static friction coefficients (Brandi, 1972; D'Angelo, 1975). Later, D'Angelo et al. (2004) measured a dynamic coefficient of sliding friction that did not vary with velocity during sinusoidal sliding, interpreting the findings as consistent with boundary lubrication. In subsequent experiments of mesothelial tissues sliding on a rotating glass plate (Loring et al., 2005), friction varied with velocity, consistent with elastohydrodynamic lubrication. In that study, shear force abruptly increased with the onset of constant rotation and then decreased progressively to a quasi-steady state during continued sliding (Fig. 1). The decrease in shear force was quicker at higher velocity, consistent with hydrodynamic pumping that increased the thickness of lubricant layer, reducing shear stress. In the present study, we test this interpretation by measuring fluid thickness at various locations between mesothelial tissue and a rotating glass plate under similar conditions. Our findings suggest that mesothelial tissue, sliding at speeds and under normal stresses characteristic of pleural tissues *in vivo*, exhibits hydrodynamic pumping previously invoked to explain redistribution of pleural fluid during breathing (Butler, et al., 1995). We infer that hydrodynamic pumping is also likely to be important to mesothelial lubrication *in vivo*.

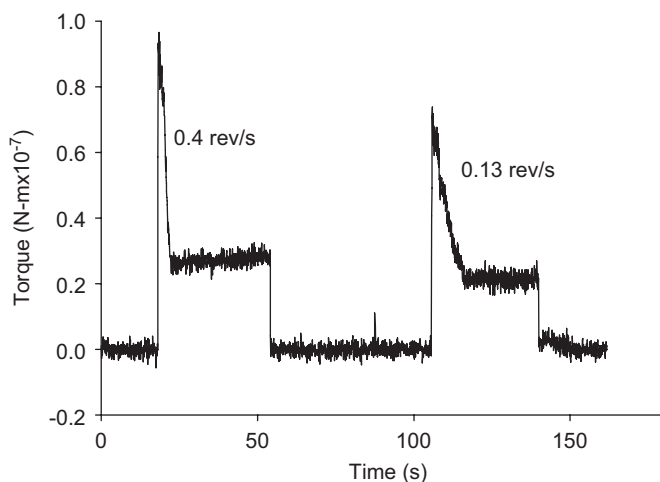


Fig. 1. Data replotted from Fig. 3 of Loring, et al. (2005). Torque applied to a disk of mesothelial tissue sliding on a glass plate rotating at rates indicated. Torque increased abruptly with the onset of motion and then progressively decreased to a steady state with continued sliding. Note that the time required to reach steady state decreased with increasing rotation rate.

2. Materials and methods

For mesothelial tissue, we used the peritoneum and underlying muscle of 30 male Sprague–Dawley rats (400–500 g) under a protocol approved by our Institutional Animal Research Committee. We used physiologic saline to simulate pleural liquid, which is a Newtonian fluid with a viscosity only 1.5 times that of water. To prevent fibrin formation on the tissue surface, heparin (5000 units i.p.) was administered 5 min before lethal anesthetic overdose (sodium pentobarbital, 200 mg/kg). Immediately after death, skin and subcutaneous tissue were reflected and the ventral abdominal wall excised, avoiding abrasion of the mesothelial surface and keeping it wet with saline.

The experimental apparatus consisted of a rotating glass plate sealed to the inner race of a ball bearing (Fig. 2). The glass plate covered with saline was rotated against a disk of mesothelial tissue glued with cyanoacrylate to the rim of an inverted metal cup (~3.7 cm diameter) that was vertically positioned with 0.1 mm resolution using a calibrated rack and pinion. The space within the metal cup over the tissue was pressurized to 2 cm H₂O to apply a uniform normal stress to the tissue surface. This created a pressure gradient driving fluid from beneath the tissue to the surrounding reservoir to simulate the non-gravitational pressure gradients within the pleural space caused by elastic deformation of the lung and chest wall (Loring et al., 2005). An inverted epifluorescence microscope measured the thickness of the layer of saline between the rotating glass and tissue (see below).

The 2 to 5-mm thick tissue sheet with the mesothelial surface facing outward was fixed under minimal tension so that it became slightly convex when pressurized. The tissue and glass plate were bathed for approximately 5 min in saline solution containing fluorescent latex microspheres (1.9 μm diameter) to allow the microspheres to adhere to glass and tissue surfaces. Unattached microspheres and solution were rinsed off before data collection. To avoid post-mortem changes in tissue properties, experiments were concluded within 2 h after death.

Images of microspheres at the focal plane appeared as small bright spots, whereas those at greater distance from the lens appeared as rings (Fig. 3). We used the linear relationship between ring radius and distance from the focal plane to measure the vertical distance between microspheres on the tissue and glass plate (one pixel diameter = 4 μm); the difference in ring size indicated the thickness of the fluid between glass and tissue. Microspheres on the tissue, glass, and in the fluid were distinguishable from images taken during rotation (Fig. 3). Microspheres on the tissue were stationary, those on glass moved in concentric circular arcs, and those that had become dislodged and were free in the fluid moved in non-circular trajectories.

In initial experiments, it became apparent that the height of the tissue-cup had a large effect on the response to rotation. (See Results.) For most studies, the height of the tissue-cup was set to a low position, ~1 mm above that at which the tissue with no pressure applied would have rested

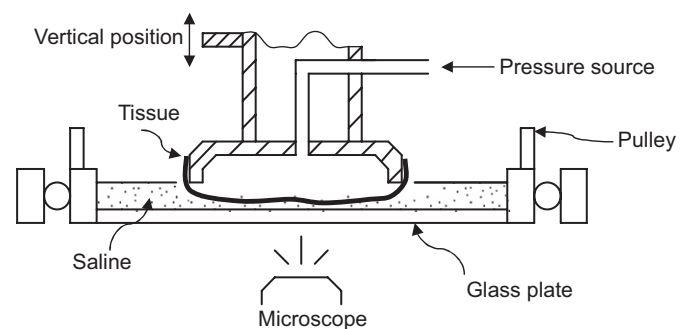


Fig. 2. Apparatus for fluid thickness measurement. The ball bearing with its glass bottom was rotated by a stepper motor and belt (not shown) over an inverted epifluorescence microscope. Tissue was fastened over the opening of an inverted metal cup (~3.7 cm diameter) and positioned close to the glass plate. Air pressure applied a spatially uniform normal stress to the top of the tissue.

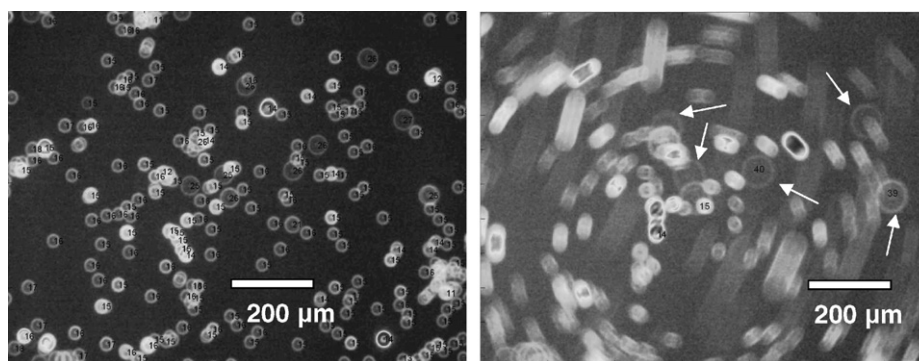


Fig. 3. Images of fluorescent microspheres on the tissue and the glass plate. Left: The glass plate is stationary before the start of rotation. Microspheres with smaller rings are closest to the focal plane, presumably on the glass, and slightly larger rings are either on the tissue surface or in the intervening fluid. Right: The glass plate is rotating at 1 rev/s. Microspheres on the glass do not change diameter and move in concentric arcs, whereas those on the tissue (arrows) are stationary and increased in size, indicating significant fluid thickening. Unattached microspheres in the fluid appear as streaked arcs that are not concentric.

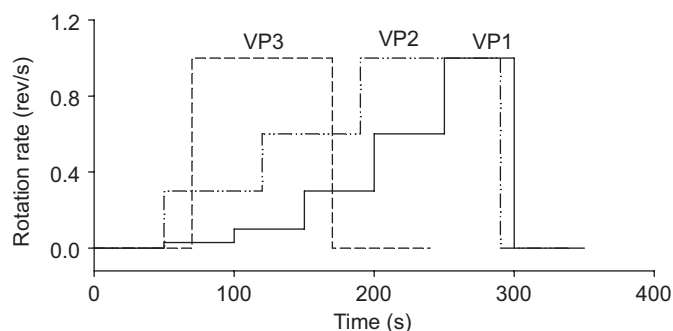


Fig. 4. Three velocity protocols used in the experiments. The maximum rotation rate was 1 rev/s, equivalent to a sliding velocity of 10 cm/s at the peripheral tissue surface.

on the glass. Saline was added or removed to leave an ~ 3 mm deep peripheral reservoir of fluid.

All runs began with application of pressure for 50–70 s prior to glass rotation, allowing the tissue to approach a quasi-steady configuration pressed close to the glass. Images were acquired every 1–2 s. To explore the influence of vertical position, the tissue-cup height was adjusted relative to an arbitrary reference, and rotation rate was varied according to velocity protocol VP1 (Fig. 4). The dependency of fluid thickness on sliding velocity was investigated by applying VP2 in clockwise and counter-clockwise directions. To explore inter-regional differences in response to rotation, we moved the apparatus relative to the microscope objective to measure thickness at different locations on the tissue surface using a single rotation rate (VP3).

3. Results

Fig. 5 shows fluid thickness measured at the center of the tissue disk during a typical experiment using VP1. Pressurization caused a decrease in fluid thickness that was not fully complete by the start of rotation. Rotation at 0.03 and 0.1 rev/s caused inconsistent changes in fluid thickness, but rotation at 0.3, 0.6, and 1 rev/s caused progressive increases in thickness to new steady states in ~ 40 , ~ 25 , and ~ 10 s, respectively. In comparing fluid thickness at different velocities, we averaged the last 10 s at each rotation rate; this approximated the steady state only at higher rotation rates. To avoid measuring thickness

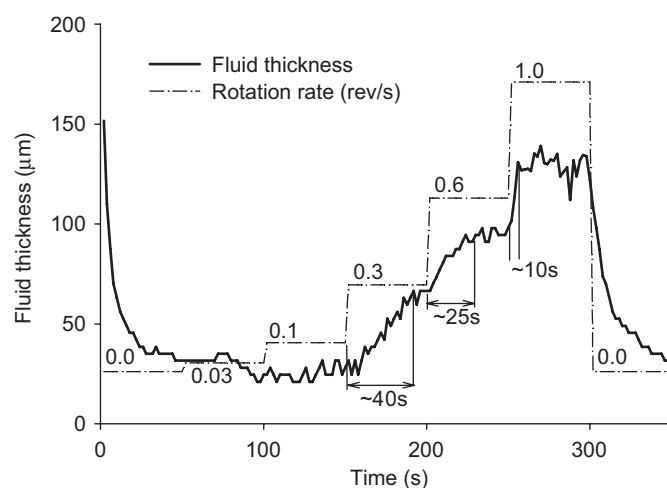


Fig. 5. Fluid thickness measurements at a low tissue-cup position. (These data are replotted in Fig. 7a at height 2.0 mm in clockwise (+) rotation.) In this test, fluid thickness increased with higher rotation rates, reaching a quasi-steady state thickness of 150 μ m after 10 s at 1 rev/s.

before the steady state, we adopted VP2, which incorporated longer periods of rotation at the three highest rotation rates.

Fig. 6 illustrates the shape of the tissue sheet, as inferred from thickness and height data, at high, intermediate, and low vertical positions (heights) of the tissue-cup. At high position, fluid near the center of the tissue was thick, and the tissue had a slightly convex shape due to the air pressure above it (Fig. 6a). At intermediate position, fluid near the center of the convex tissue surface was thin while that in peripheral regions remained thick (Fig. 6b). At low cup position, a wide area of the tissue sheet was pressed close to the glass by pressure above it (Fig. 6c). However, microscopic unevenness of the flattened tissue surface resulted in spatial variations in fluid thickness and variable thickness at the center.

Fig. 7 shows fluid thickness as a function of rotation rate at several tissue-cup positions in three experiments. Without rotation (rate 0), changes in the vertical position of the

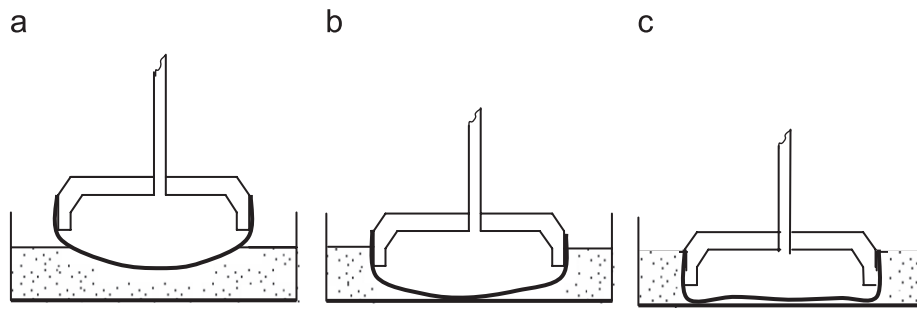


Fig. 6. Schematic illustration of the effect of tissue-cup position on tissue conformations: (a) High; (b) Medium; (c) Low (See text.)

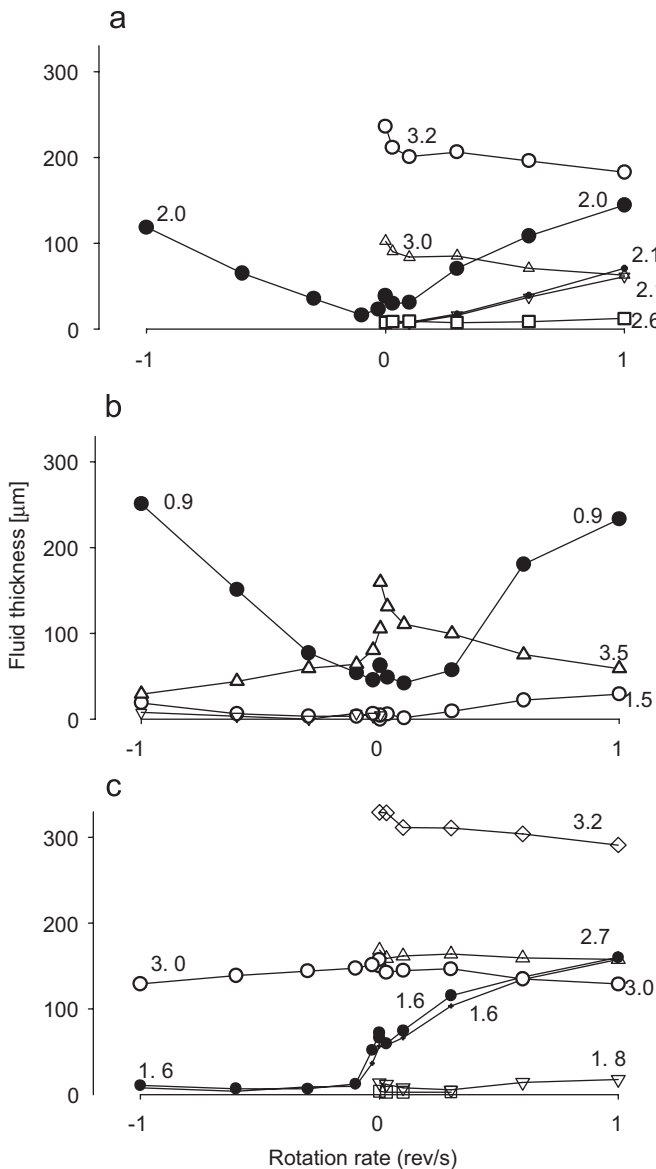


Fig. 7. Fluid thickness measured at different tissue-cup heights and rotation rates, clockwise positive. Numbers indicate vertical cup position (mm) above a reference; lowest numbers are closest to the glass. Each point represents an average of thickness during the last 10 s of rotation at each rate. At high tissue-cup position, all runs showed a decrease in fluid thickness in both directions. At low tissue-cup positions (solid symbols), (a) and (b) showed similar behavior in both rotational directions, whereas (c) showed opposite behavior.

tissue-cup corresponded to changes in the thickness of the fluid only at high cup positions where the tissue was not deformed by contact or near contact with the glass. For example, in Fig. 7c, when cup position was lowered 0.2 mm from 3.2 to 3.0 mm, fluid depths decreased 180 μm from 329 to 149 μm , whereas when the cup was further lowered to 2.7 mm, fluid depth decreased little because of flattening of the tissue sheet. At lower cup positions, fluid thickness did not correspond with cup height, presumably because the uneven tissue surface, pressed against the glass, did not move with the cup. In 28 experiments with the tissue-cup in its lowest position, fluid thickness at the center ranged from approximately 0 μm (less than 4 μm) to 144 μm (mean 33 μm , median 28 μm), reflecting microscopic unevenness of the tissue surface.

With glass rotation, the change in fluid thickness was critically dependent on cup height. As shown in Fig. 7, at high cup positions (e.g., 3.2 mm in Fig. 7a), fluid thickness was high and did not change appreciably at low rotation rates (e.g., 0.03 and 0.1 rev/s). (The apparent decrease in thickness at low rates is probably due to progressive thinning unrelated to rotation, as in Fig. 5.) At high rotation rates (0.6 and 1 rev/s), fluid thickness always decreased (e.g., Fig. 7a, height 3.2 mm). At an intermediate cup position, fluid was thin and usually remained thin with rotation or thickened slightly (e.g., Fig. 7a, height 2.6 mm; Fig. 7b, height 1.5 mm; and Fig. 7c, height 1.8 mm). In contrast, at low cup position, fluid thickness frequently increased markedly with rotation (e.g., Fig. 7a, height 2.0 mm; Fig. 7b, height 0.9 mm; Fig. 7c, height 1.6 mm).

For determining the effects on fluid thickness of rotation rate, direction, and location on the tissue, the cup was set at a low position. In 28 experiments, we evaluated the effects on fluid thickness at the center of rotation at 1 rev/s in 2 directions. In 49 of 56 observations, thickness increased (average change +46 μm , SD 55 μm , range -62 to +195 μm , $P < 0.0001$ by paired t -test).

In 7 of the 56 observations above, thickness decreased progressively with increasing rate as in Fig. 7c in the counter-clockwise direction (solid symbols). These results were reproducible as shown in repeated runs in Fig. 7c at height 1.6 mm. To assess the degree to which thickness changes were different in different directions, we calculated a difference ratio (DR) as the absolute difference between

thickness changes in clockwise and counter-clockwise directions divided by the average change: $DR = |(\Delta Th_{CW} - \Delta Th_{CCW}) / (0.5 * (\Delta Th_{CW} + \Delta Th_{CCW}))|$. We chose a threshold value, $DR \geq 0.5$, to indicate a substantial difference in response. By this criterion, 18 of 28 experiments showed fluid thickening that was substantially different in magnitude or sign in the two directions.

To explore regional differences in the response to rotation, we repositioned the apparatus on the microscope

to measure fluid thickness in more peripheral regions of the tissue disk. In Fig. 8, average fluid thicknesses are plotted before and during rotation in each direction. Five of the experiments appear to show similar changes in thickness at different locations, whereas six appear to show substantially different changes at different locations. We evaluated the random effect of tissue sample and the effect of central versus non-central location using ANOVA (JMP, SAS Institute, Cary, NC, USA). Variations in fluid thickness

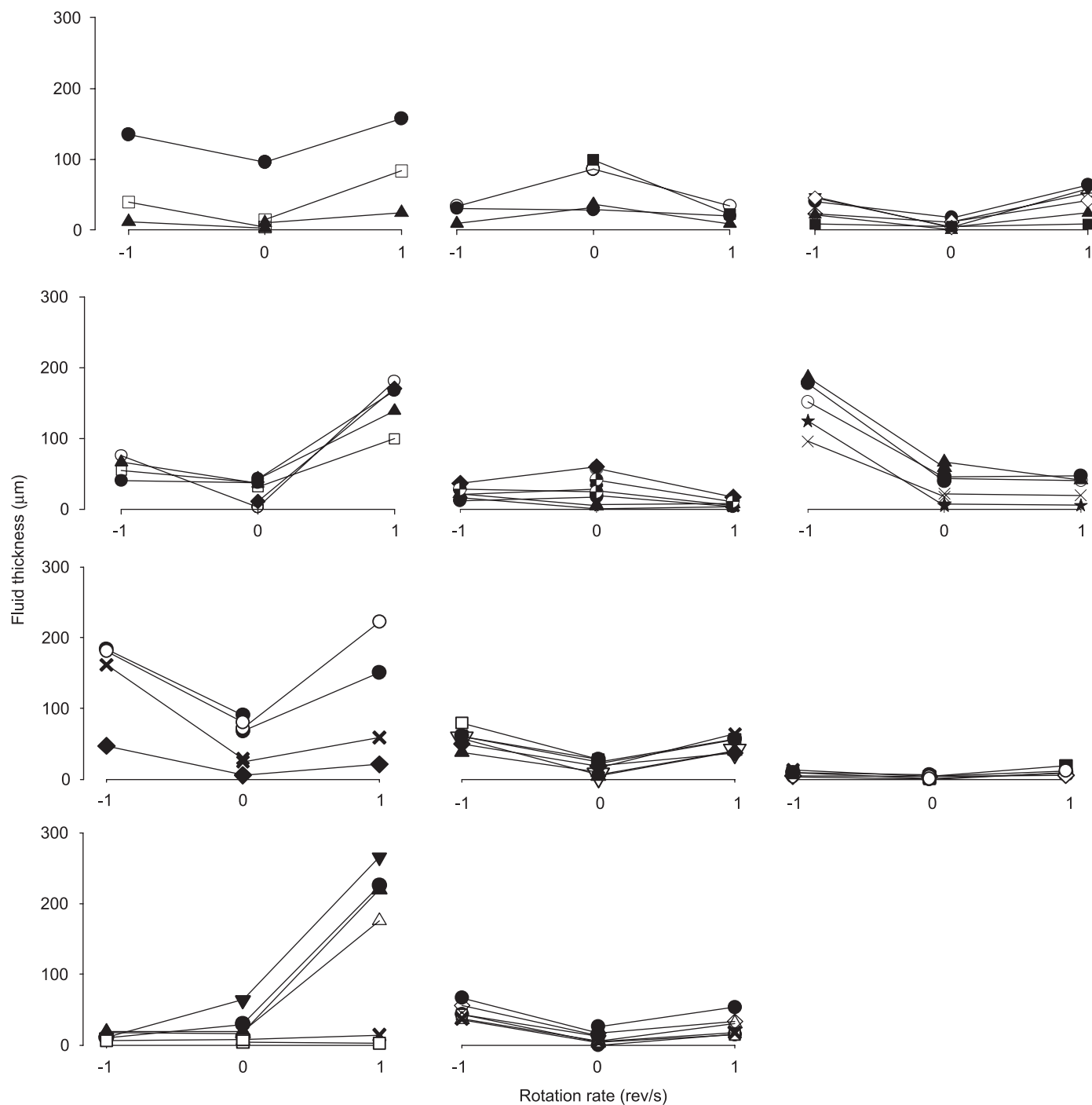


Fig. 8. Fluid thickness measurements at selected locations on 11 tissue samples, clockwise positive. Each figure represents one tissue sample, each symbol represents one location; the central position is indicated by a filled circle. The vertical position of the tissue-cup was constant in each experiment.

with rotation were significantly related to tissue sample ($P < 0.0001$) but not to central versus non-central location ($P = 0.42$).

4. Discussion

In general, fluid thickness increased with increasing rotation rate. The time to reach steady-state thickness decreased with increasing rotation rate (Fig. 5), consistent with a similarly timed decrease in torque observed in a previous investigation (Loring et al., 2005). These results suggest a hydrodynamic mechanism that pumped fluid against the global pressure gradient from the surrounding reservoir into the space under the tissue, increasing the thickness of the fluid layer.

4.1. Critique of method and comparison with the pleural space

How do our observations of peritoneal tissue pressed against a rotating glass plate apply to lungs sliding against the chest wall during breathing? In the pleural space, pressure *per se* varies temporally and spatially, but it is the gradients in pressure caused by spatial, non-gravitational variations in pleural surface stress that affect pleural lubrication. Such gradients arise from the inevitable difference between the unconstrained shape of the lung and that of the chest wall. For example, pressure beneath a rib that indents the lung would be higher than pressure beneath an adjacent intercostal space. Fig. 9 shows such spatial variation in pleural liquid thickness in a quick-frozen specimen. We previously estimated an upper limit of the normal stress (pressure) arising from such small-scale indentations of the relatively soft lung and chest wall (modulus of elasticity ~ 500 Pa) to be approximately 2 cm H₂O (Loring, et al., 2005). Pressure gradients resulting from such pressures would tend to drive pleural liquid from regions of relatively high pressure to surrounding regions of lower pressure and, given enough time, would result in physical contact between the opposing surfaces. Hydrodynamic pumping caused by sliding, as demonstrated in our experiments, could oppose this effect by moving pleural liquid from regions with relatively thick layers of fluid at lower pressure to regions of thinner liquid at higher pressure, thus maintaining separation of pleural surfaces in regions that would statically be in contact.

Although we demonstrated hydrodynamic pumping using continuous motion, the same phenomenon would be seen during reciprocating motion as in breathing. Fluid translocation caused by sliding persists for a time after sliding stops (Fig. 5), and physical, computational and mathematical studies have confirmed that reciprocating and continuous sliding cause similar steady-state effects (Butler et al., 1995; Gouldstone et al., 2003).

The pleural cavity is a closed space containing pleural liquid (about 2 ml in humans) whose volume is essentially

constant in a period of a few minutes and well regulated over many hours or days (Lai-Fook, 2004). As a result, redistribution of fluid from thick to thin regions in the pleural space by reciprocating sliding results in a relatively even fluid layer of limited thickness (Gouldstone et al., 2003). By contrast, in our experiments, the effectively infinite peripheral reservoir and compliant liquid-filled space beneath the tissue allowed hydrodynamic pressure gradients to cause large changes in translocations of fluid and spatial variations in fluid thickness. Fig. 9 shows an example of the unevenness of mesothelial surface when the tissue is unconstrained and the comparative smoothness of the surface of pleural tissue *in situ*.

The fluid thickening we observed at the center of the tissue sheet was almost certainly due to highly local hydrodynamic pressures generated in more peripheral regions. Our reasoning is as follows: positive or negative hydrodynamic pressure is generated beneath any inclined surface sliding in lubricant and is proportional to velocity and strongly negatively related to fluid thickness (Batchelor, 2005). Any uneven surface, such as the tissue in our experiments, is a series of inclined surfaces producing highly local pressure increases and decreases, which, depending on their spatial distribution, could pump fluid over long distances (Fig. 9). The peripheral regions of the tissue sheet, where sliding velocities are greater, would be those able to generate local hydrodynamic pressures sufficient to cause global fluid movement towards (or away from) the center, often against the global pressure gradient. At the highest rotation rate, sliding velocity at periphery was 9 cm/s, which is similar to that of the caudal lung during rapid breathing.

Other potential hydrodynamic mechanisms of fluid thickness change include local shear-induced smoothing of asperities, with fluid translocation between neighboring regions of greater and lesser fluid thickness (Gouldstone, et al., 2003). However, we observed similar thickness changes at different locations (Fig. 8), and at 1 rev/s fully 10 revolutions were required to reach steady state (Fig. 5), suggesting hydrodynamic pumping rather than smoothing of asperities. In peripheral regions, elastohydrodynamic lift generation could also increase thickness. Elastic structures sliding in lubricant are deformed by hydrodynamic pressures so as to generate lift (Skotheim and Mahadevan, 2005). We have recently demonstrated elastohydrodynamic lift using a three-dimensional finite element model of an uneven elastic solid sliding against a rotating surface as in this study (Moghani et al., 2007).

Other mechanisms of pleural lubrication have been proposed. Miserocchi and Agostoni (1971) discussed the possibility that mesothelial cells or white cells in pleural liquid could act as ball bearings to reduce friction. Agostoni (1986) suggested that boundary lubrication may be assisted by hyaluronan, and Hills (1992) have suggested that oligolamellar surfactants in the pleural space act as dry lubricants. Both hyaluronan and phospholipids are present only at very low concentrations in pleural liquid, and their

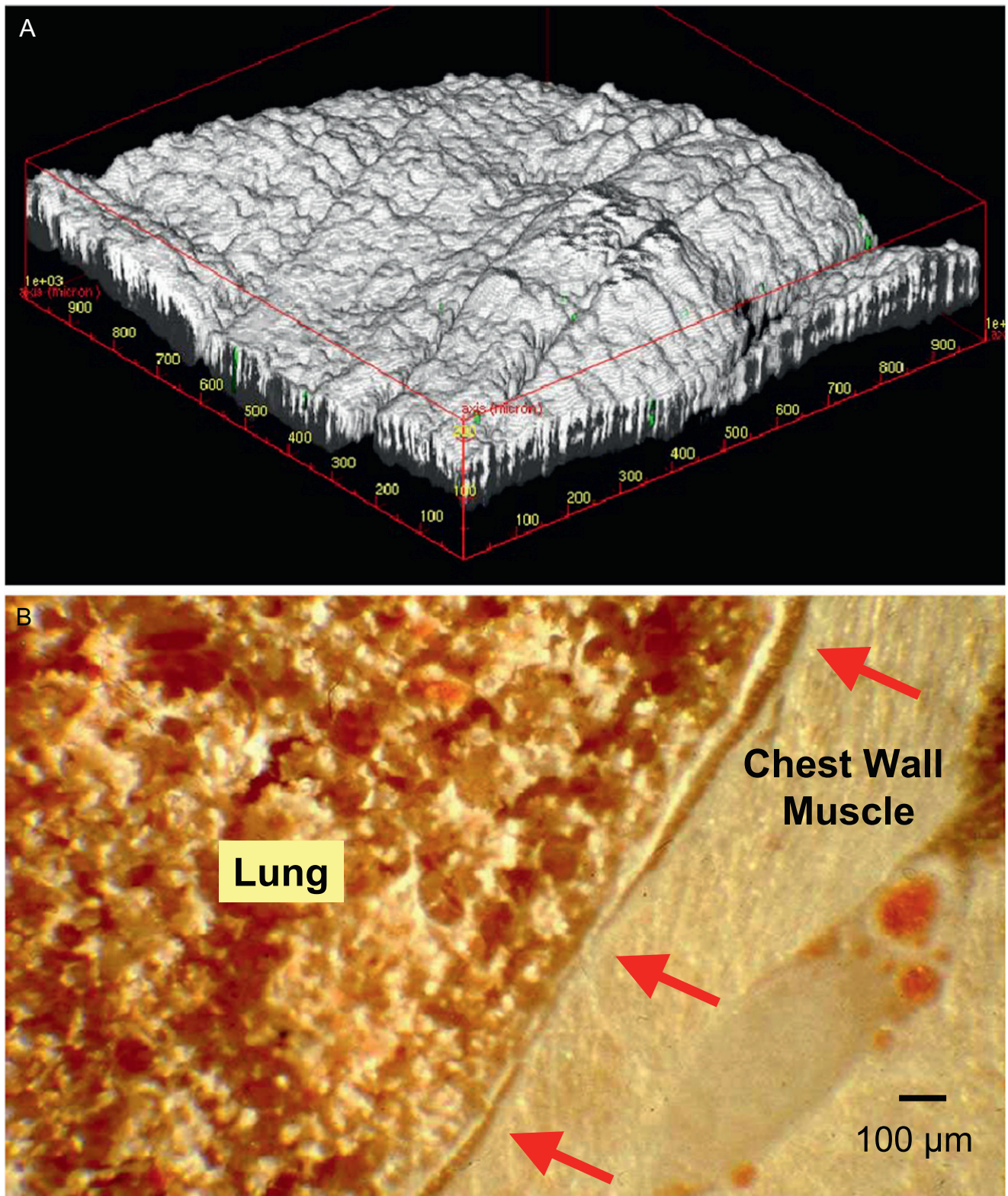


Fig. 9. Surface topography of mesothelial tissues. (A) Surface rendering of a laser scanning confocal micrograph of a 1×1 mm area; the pleural surface of rat diaphragm in oblique view. The tissue, which was submerged in saline and unstressed, shows substantial surface roughness. Tissues under tension or smoothed by sliding against flat glass would have been less rough. Numbers at the edges indicate $100 \mu\text{m}$ intervals. (B) Chest wall and lung of a rat quick-frozen in liquid nitrogen immediately after death. The pleural liquid-ice layer (arrows) varies from about $40 \mu\text{m}$ to less than $5 \mu\text{m}$. Compared with the unstressed mesothelial surface in (A), the pleural surfaces are relatively smooth, and the fluid layer is relatively even due to redistribution of a fixed fluid volume during breathing.

importance in pleural lubrication has been considered speculative (Lai-Fook, 2004).

In a variety of other biological systems, hydrodynamic lubrication is evident (Jin and Dowson, 2005). Under conditions of high normal stress and low sliding velocity such as those in joints, elastohydrodynamic lubrication may be inadequate. Joint lubrication is facilitated by macromolecular components of cartilage that apparently act like hydrated gels whose sliding surfaces repel each other, providing an aqueous layer of hydrated polymer chains that greatly reduces friction (see the review by Gong, 2006). Glycoproteins on mesothelial cells may be important in mesothelial lubrication. In our experiments, however, normal stresses were relatively low, and the fluid layer separating the sliding surfaces was probably too thick to allow the chemical repulsion between surfaces characteristic of hydrated gels.

A prominent feature of our findings was the variation among tissue samples in response to glass rotation, which was similar to the variation in frictional behavior seen previously (Loring et al., 2005). Such variation is probably due to different surface topography of individual tissue sheets (see Fig. 9) causing differing local hydrodynamic pressures and global changes in fluid thickness. Similarly, surface unevenness asymmetrical with respect to direction of rotation would result in different effects of clockwise and counter-clockwise rotation. Although in most experiments fluid thickness increased with rotation, with the tissue-cup high, fluid thickness invariably decreased at high rotation rates regardless of direction of rotation and tissue sample (Fig. 7). This was quantitatively consistent with an inertial (centrifugal) effect of the rotating fluid.

Mesothelial tissue sliding on glass should exhibit elastohydrodynamic lubrication and pumping similar to that of tissue sliding on tissue; both cause shear-flow in a fluid channel with non-parallel boundaries and hydrodynamic pressure generation. Skotheim and Mahadevan (2005) showed that a soft object sliding on a hard surface, a hard object sliding on a soft surface, and a soft object sliding on a soft surface share the same governing equations. Furthermore, tissue sliding on tissue and tissue sliding on glass both exhibit velocity-dependent friction suggestive of elastohydrodynamic lubrication (Loring et al., 2005).

3.2. Previous studies

Several recent investigations on pleural lubrication have demonstrated elastohydrodynamic lubrication in models (Butler et al., 1995; Gouldstone et al., 2003; Moghani et al., 2007) and *in vitro* (Loring et al., 2005). However, a recent study by D'Angelo et al. (2004) found the friction coefficient of mesothelial tissues to be invariant with velocity during sinusoidal sliding at 0.3–2 Hz with a fixed excursion of 1 cm, consistent with boundary lubrication. Shear-induced fluid redistribution in this experiment and *in vivo* would be expected to persist during velocity reversals

(Gouldstone et al., 2003), possibly confounding the interpretation of oscillatory responses. The differences between these results remain unexplained.

In experiments *in vivo*, Wang and Lai-Fook (1993, 1997) demonstrated that increasing tidal volume or breathing frequency caused the thickness of the pleural space over the costal surface of the lungs to increase. They concluded that fluid was pumped from the lobar margins, where the pleural space is relatively thick and the pressure statically low, to the pleural space overlying the lung, where the pressure is statically higher. This is consistent with hydrodynamic pumping of fluid from a peripheral reservoir against the global pressure gradient.

Conflict of interest statement

The authors have no financial or other interest that could affect the objectivity with which they approach the subject matter of this investigation.

Acknowledgments

The authors thank Dr. Richard E. Brown for many of the methods and insights presented in this report. Fig. 9A was prepared by Dr. Brown with the Bioimaging Facility at Harvard School of Public Health. Current address of B.F.: Department of Physics, University of Erlangen-Nuremberg, Henkestrasse 91, D-91052 Erlangen, Germany.

This work was supported in part by HL63737 from the National Institutes of Health.

References

- Adamson, A.W., 1982. Friction and lubrication-adhesion. In: Physical Chemistry of Surfaces. Wiley, New York, pp. 402–432 (Chapter 12).
- Agostoni, E., 1986. Mechanics of the pleural space. In: Macklem, P.T., Mead, J. (Eds.), Handbook of Physiology. American Physiological Society, Bethesda, MD, pp. 531–559.
- Agostoni, E., D'angelo, E., 1991. Pleural liquid pressure. *Journal of Applied Physiology* 71, 393–403.
- Batchelor, G.K., 2005. An Introduction to Fluid Dynamics. Cambridge University Press, New York, USA, pp. 219–222.
- Brandi, G., 1972. Frictional forces at the surface of the lung. *Bulletin Physiopathol. Respir. (Nancy)* 8, 323–336.
- Butler, J.P., Huang, J., Loring, S.H., Lai-Fook, S.J., Wang, P.M., Wilson, T.A., 1995. Model for a pump that drives circulation of pleural fluid. *Journal of Applied Physiology* 78, 23–29.
- D'angelo, E., 1975. Stress-strain relationships during uniform and non uniform expansion of isolated lungs. *Respiratory Physiology* 23, 87–107.
- D'angelo, E., Loring, S.H., Gioia, M.E., Pecchiari, M., Moscheni, C., 2004. Friction and lubrication of pleural tissues. *Respiratory Physiology & Neurobiology* 142, 55–68.
- Dowson, D., 1969. Transition to boundary lubrication from elastohydrodynamic lubrication. In: Ling, F.F., Klaus, E.E., Fein, R.S. (Eds.), Boundary Lubrication: an Appraisal of World Literature. The American Society of Mechanical Engineers, New York, pp. 229–240 (Chapter 11).
- Gong, J.P., 2006. Friction and lubrication of hydrogels—its richness and complexity. *Soft Matter* 2, 544–552.

- Gouldstone, A., Brown, R.E., Butler, J.P., Loring, S.H., 2003. Elastohydrodynamic separation of pleural surfaces during breathing. *Respiratory Physiology & Neurobiology* 137, 97–106.
- Hills, B.A., 1992. Graphite-like lubrication of mesothelium by oligolamellar pleural surfactant. *Journal of Applied Physiology* 73, 1034–1039.
- Jin, Z.M., Dowson, D., 2005. Elastohydrodynamic lubrication in biological systems. *Journal of Engineering Tribology* 211, 367–380.
- Lai-Fook, S.J., 1987. Mechanics of the pleural space: fundamental concepts. *Lung* 165, 249–267.
- Lai-Fook, S.J., 2004. Pleural mechanics and fluid exchange. *Physiological Reviews* 84, 385–410.
- Lai-Fook, S.J., Rodarte, J.R., 1991. Pleural pressure distribution and its relationship to lung volume and interstitial pressure. *Journal of Applied Physiology* 70, 967–978.
- Loring, S.H., Brown, R.E., Gouldstone, A., Butler, J.P., 2005. Lubrication regimes in mesothelial sliding. *Journal of Biomechanics* 38, 2390–2396.
- Miserocchi, G., Agostoni, E., 1971. Contents of the pleural space. *Journal of Applied Physiology* 30, 208–213.
- Moghani, T., Butler, J.P., Lin, J.L., Loring, S.H., 2007. Finite element simulation of elastohydrodynamic lubrication of soft biological tissues. *Computers & Structures* 85, 1114–1120.
- Skotheim, J.M., Mahadevan, L., 2005. Soft lubrication: the elastohydrodynamics of nonconforming and conforming contacts. *Physics of Fluids* 17.
- Wang, P.M., Lai-Fook, S.J., 1993. Effect of ventilation frequency and tidal volume on pleural space thickness in rabbits. *Journal of Applied Physiology* 75, 1836–1841.
- Wang, P.M., Lai-Fook, S.J., 1997. Effect of mechanical ventilation on regional variation of pleural liquid thickness in rabbits. *Lung* 175, 165–173.